

Current oscillation in GaN-HEMTs with p-GaN islands buried layer for terahertz applications

Wen-Lu Yang(杨文璐), Lin-An Yang(杨林安)†, Fei-Xiang Shen(申飞翔), Hao Zou(邹浩),Yang Li(李杨), Xiao-Hua Ma(马晓华), and Yue Hao(郝跃)

Citation: Chin. Phys. B, 2022, 31 (**5**): 058505. DOI: 10.1088/1674-1056/ac2b1f
Journal homepage: http://cpb.iphy.ac.cn; http://iopscience.iop.org/cpb

What follows is a list of articles you may be interested in

Impact of oxygen in electrical properties and hot-carrier stress-induced degradation of GaN high electron mobility transistors

Lixiang Chen(陈丽香), Min Ma(马敏), Jiecheng Cao(曹杰程), Jiawei Sun(孙佳惟), Miaoling Que(阙妙玲), and Yunfei Sun(孙云飞)

Chin. Phys. B, 2021, 30 (**10**): 108502. DOI: 10.1088/1674-1056/ac1efd

Performance analysis of GaN-based high-electron-mobility transistors with postpassivation plasma treatment

Xing-Ye Zhou(周幸叶), Xin Tan(谭鑫), Yuan-Jie Lv(吕元杰), Guo-Dong Gu(顾国栋), Zhi-Rong Zhang(张志荣), Yan-Min Guo(郭艳敏), Zhi-Hong Feng(冯志红), and Shu-Jun Cai(蔡树军)

Chin. Phys. B, 2021, 30 (**2**): 028502. DOI: 10.1088/1674-1056/abb7f6

Influences of increasing gate stem height on DC and RF performances of InAlAs/InGaAs InP-based HEMTs

Zhi-Hang Tong(童志航), Peng Ding(丁芃), Yong-Bo Su(苏永波), Da-Hai Wang(王大海), and Zhi Jin(金智)

Chin. Phys. B, 2021, 30 (**1**): 018501. DOI: 10.1088/1674-1056/abb30d

A 2DEG back-gated graphene/AlGaN deep-ultraviolet photodetector with ultrahigh responsivity

Jinhui Gao(高金辉), Yehao Li(李叶豪), Yuxuan Hu(胡宇轩), Zhitong Wang(王志通), Anqi Hu(胡安琪), and Xia Guo(郭霞)\ccclink

Chin. Phys. B, 2020, 29 (**12**): 128502. DOI: 10.1088/1674-1056/abb3eb

Enhancement of radiation hardness of InP-based HEMT with double Si-doped plane

Ying-Hui Zhong(钟英辉), Bo Yang(杨博), Ming-Ming Chang(常明铭), Peng Ding(丁芃), Liu-Hong Ma(马刘红), Meng-Ke Li(李梦珂), Zhi-Yong Duan(段智勇), Jie Yang(杨洁), Zhi Jin(金智), Zhi-Chao Wei(魏志超)

Chin. Phys. B, 2020, 29 (**3**): 038502. DOI: 10.1088/1674-1056/ab6962

Current oscillation in GaN-HEMTs with p-GaN islands buried layer for terahertz applications

Wen-Lu Yang(杨文璐), Lin-An Yang(杨林安)†, Fei-Xiang Shen(申飞翔), Hao Zou(邹浩), Yang Li(李杨), Xiao-Hua Ma(马晓华), and Yue Hao(郝跃)

State Key Discipline Laboratory of Wide Band-gap Semiconductor Technology, School of Microelectronics, Xidian University, Xi'an 710071, *China*

(Received 29 June 2021; revised manuscript received 25 September 2021; accepted manuscript online 29 September 2021)

A GaN-based high electron mobility transistor (HEMT) with p-GaN islands buried layer (PIBL) for terahertz applications is proposed. The introduction of a p-GaN island redistributes the electric field in the gate–drain channel region, thereby promoting the formation of electronic domains in the two-dimensional electron gas (2DEG) channel. The formation and regulation mechanism of the electronic domains in the device are investigated using Silvaco-TCAD software. Simulation results show that the 0.2 μm gate HEMT with a PIBL structure having a p-GaN island doping concentration (N_p) of 2.5×10^{18} cm^{-3}–3×10^{18} cm^{-3} can generate stable oscillations up to 344 GHz–400 GHz under the gate–source voltage (V_{gs}) of 0.6 V. As the distance (D_p) between the p-GaN island and the heterojunction interface increases from 5 nm to 15 nm, the fundamental frequency decreases from 377 GHz to 344 GHz, as well as the ratio of oscillation current amplitude of the fundamental component to the average component I_{f1}/I_{avg} ranging from 2.4% to 3.84%.

Keywords: p-GaN island, high electron mobility transistor (HEMT), AlGaN/GaN, electron domain

PACS: 85.30.Mn, 05.10.Ln, 61.72.uj, 52.70.Gw **DOI:** 10.1088/1674-1056/ac2b1f

1. Introduction

For applications of terahertz (THz) technology, much research has been devoted to finding efficient solid-state terahertz sources at room temperature.[1,2] As a typical structure based on heterojunction, HEMTs have gained widespread attention on account of their excellent properties such as high breakdown electric field, high electron velocity and concentration, and is usually studied as an amplifier.[3,4] In recent years, with the progress of material growth and device manufacturing technology, HEMTs have been considered as a possible THz source.

There are two types of mechanisms for generating THz oscillation in HEMTs. One is the plasma instability in the two-dimensional electron gas (2DEG) channel, which can result in high-frequency oscillations above 1 THz. The other is the Gunn effect. Under the action of a high electric field, a part of the electrons transition into the high-energy valley, thereby increasing effective mass and decreasing mobility. This contributes to part of the electron accumulation, thus forming Gunn domains.[2] Gunn domains cause an oscillating output current and some experiments and simulations have reported current instability in HEMTs, in which the current oscillation frequency even reaches the THz range.[5] Compared to the vertically structural Gunn diodes, HEMTs advantageously are compatible with traditional planar device process.[6,7] For GaN-based HEMTs, the 2DEG with a high electron concentration induced by the polarization effect is very beneficial for the formation of electronic domains and makes devices have good combined frequency–power performance.[8] Studies on Gunn oscillation in GaN-based planar Gunn devices have achieved significant results, and the frequency of the devices has approached the THz range.[9–11]

However, there are still some challenges in using GaN-based HEMTs as Gunn oscillation sources. The high electric field region at the edge of the gate is too narrow, making it difficult to obtain a stable oscillating current in traditional GaN-based HEMTs. The method of applying a large gate bias voltage to expand the high electric field region to trigger the formation of Gunn domains may cause large leakage currents and increase the risk of device damage. In addition, to achieve terahertz oscillation, the oscillation channel length of these Gunn devices is usually less than 1 μm. This not only reduces the breakdown voltage of the device but also increases the difficulty of the process, especially the deposition of ohmic electrodes.[12]

In this paper, a novel GaN-based HEMT with a p-GaN islands buried layer (PIBL) is proposed based on the Silvaco-TCAD simulation. By introducing the p-GaN island in the buffer under the channel of the gate–drain region, the electric field in the 2DEG channel can be redistributed to make it more conducive to trigger the formation of electronic domains. We investigate the mechanism of generation and regulation of the formation of electronic domains in the channel, particularly the influence of the position of p-GaN island and the applied V_{gs} on the electronic domain and oscillation frequency.

†Corresponding author. E-mail: layang@xidian.edu.cn

© 2022 Chinese Physical Society and IOP Publishing Ltd

2. Device structure and parameters for simulation

The schematic diagrams of AlGaN/GaN HEMTs with the PIBL structure used in our simulation are shown in Fig. 1, and detailed device parameters are listed in Table 1. The thickness and length of the p-GaN island affect the electric field strength and the length of the domain-forming region and thereby the formation of electronic domains. In order to obtain a stable oscillating current, we set the p-GaN island to have the length $L_p = 0.3$ μm.

Table 1. Device structure parameters in the simulation.

Parameter	Value
Gate–source distance (L_{gs}) (μm)	0.6
Gate length (L_g) (μm)	0.2
Gate–drain distance (L_{gd}) (μm)	1.2
Gate metal work function (eV)	5.1
Source/drain metal work function (eV)	3.93
p-GaN island length (L_p) (μm)	0.3
p-GaN island thickness (T_p) (nm)	10
p-GaN doping concentration (N_p) (10^{18} cm^{-3})	3
AlGaN layer thickness (T_a) (nm)	25
GaN buffer layer thickness (T_g) (μm)	0.1
Distance between p-GaN island and AlGaN layer (D_p) (nm)	5–15

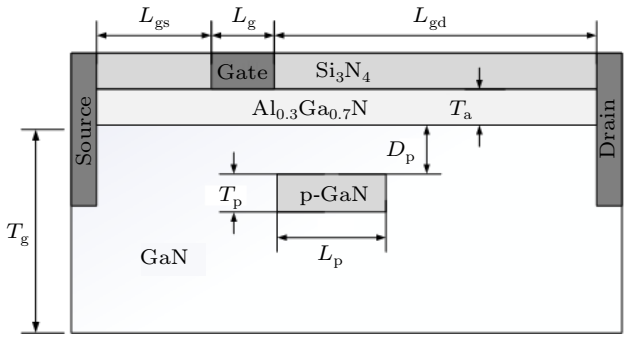


Fig. 1. Schematic of AlGaN/GaN HEMTs with PIBL.

The source and drain electrodes are vertical ohmic contact electrodes located on both sides of the device and are in contact with the 2DEG channel. This type of source/drain electrodes fabricated by re-growth technology is commonly used in high-frequency GaN-based HEMTs[13–15] since it can provide excellent control of the channel electric field. The significant reduction of the on-resistance can also promote the generation and propagation of electronic domains. In our simulation, the ohmic contact resistance is set as 0.4 Ω/mm. The p-GaN island is located in the GaN buffer layer below the gate edge and has floating potential. The p-GaN island-shaped buried layer structure in this paper can be achieved by using the method reported with the GaN-based current aperture vertical electron transistor (CAVET).[16–18] Firstly, dry etching technology is applied to selectively etch the p-GaN layer to form the island at the designated position. Then, the GaN layer is grown to fill the etched trench via the use of re-growth technology. Finally, low-temperature molecular beam epitaxy (MBE) technology is adopted to grow an AlGaN/GaN heterojunction. The p-GaN island region is uniformly doped, and the thickness of the p-GaN island is defined as 10 nm in our numerical simulation. In realistic processing, some methods can be used to reduce the influence of Mg diffusion into the 2DEG channel, such as regrowing the AlGaN/GaN layer above the p-GaN island in a low-temperature environment using MBE technology[19,20] or increasing the distance between the PIBL and the heterojunction interface.

Donor-like defects/impurities inevitably exist at the interface of the p-GaN island and surrounding GaN. The state at the p-GaN/GaN interface, mainly introduced by ion implantation and secondary epitaxy, should be considered in the simulation.[21,22] In the simulation, we set the trapped charge density to be 2.8×10^{12} cm^{-2} with location at the p–n junction interface ($E - E_v = 3.2$ eV).[23,24] A previous article reports that optimizing the interface cleaning and growth conditions can reduce the interface state density.[25]

Non-local transport effects such as the velocity overshoot have great influence on sub-micron devices and should be considered in simulations. Therefore, we adopt the energy-balance (E-B) transport model instead of the traditional drift–diffusion (D–D) transport model in the simulation, the E-B model being a non-local model widely used in high-frequency and small-sized devices. Due to the buried p–n junction in the device, Shockley–Read–Hall (SRH) model is also included in our simulation.

Table 2. Transport model parameters at room temperature (T = 300 K).[9,26,27]

V_{sat} (cm/s)	E_c (V/cm)	n1n.gansat
2.6×10^7	1.311×10^5	9.1
n2n.gansat	ann.gansat	μ_0 (cm^2/V·s)
0.649	4.057	1274

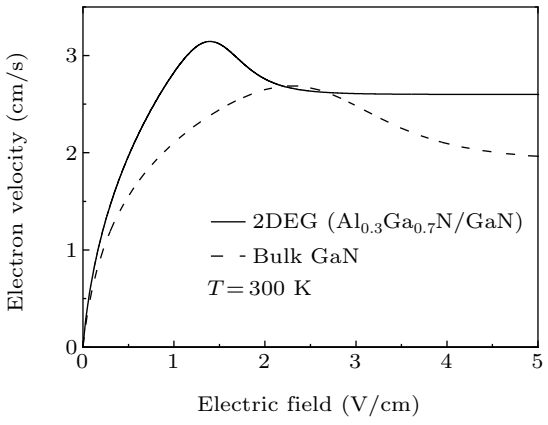


Fig. 2. Velocity versus electric field dependence of 2DEG and bulk GaN.

To reasonably characterize 2DEG in the AlGaN/GaN heterostructure, we employ the fitting parameters of the mobil-

ity model obtained from Monte Carlo simulations and experiments in the simulation. The effects of the interface state, velocity overshoot and carrier scattering mechanisms are all taken into account.[26] The velocity–electric field dependence parameters at room temperature ($T = 300$ K) used in our simulation are listed in Table 2.[9,26,27] Figure 2 plots the velocity-versus-electric field dependence of 2DEG. Compared with bulk GaN, 2DEG shows a higher peak drift velocity and a higher saturation drift velocity.

In addition, we use the method of transient simulation to generate a stable current oscillation waveform instead of the circuit-level simulation, mounting the device into the RLC network, where the maximum time step is 0.1 ps and the ramping rate is 33 V/ns. The fast Fourier algorithm is used to analyze the oscillating current waveform obtained at each voltage bias point.

3. Simulation results and discussion

Figures 3 and 4 show the transient simulation results of conventional HEMTs and PIBL HEMTs under the same voltage bias conditions. The distribution of the electric field and electron concentration in the channel are shown in Figs. 5 and 6, where the gate bias voltage $V_{gs} = 0.6$ V and the drain bias voltage $V_{ds} = 12.5$ V. Figure 3 gives a comparison of the transient drain current for GaN-HEMTs with and without a PIBL structure. In the proposed HEMT, an evident oscillation appears like a Gunn oscillation, while the conventional HEMT maintains a stable output current. A lower drain current for the PIBL structural HEMT is attributed to the PIBL structure reducing the local electron concentration in the 2DEG channel. The frequency spectrum of the oscillation current calculated by fast Fourier analysis is shown in Fig. 4, yielding an available fundamental frequency at around 377 GHz, accompanied by the ratio of the oscillation current amplitude of the fundamental component to the average component $I_{f1}/I_{avg} \approx 3.84\%$. The frequency is far higher than the f_T and f_{MAX} of the equivalent conventional GaN HEMT with a gate length of 0.2 μm.[3] In previous articles, the p-GaN buried layer was often used in CAVET as a current blocking layer to adjust the distribution of the bulk electric field.[14–16,28,29] In this paper, however, PIBL is used to adjust the local electric field distribution which aims to form a perturbation field at the edge of the gate.

The p-GaN region and the surrounding GaN material form a p–n junction, thus depleting part of the 2DEG. The p-GaN island reduces the electron concentration in the 2DEG channel above it, thereby forming a local high resistance region. Most of the drain voltage is applied to this high resistance region so that a relatively wide high electric field region is formed in the channel, which makes it easier for electrons to transition into a high-energy valley, thereby triggering the formation of Gunn domains, as shown in Fig. 5. Due to the low mobility of electrons in the high energy valley, the electron drift velocity is low, which causes the accumulation of electrons. The electrons behind the domain arrive at a higher velocity, making the domain grow. Simultaneously, the drift velocity of electrons within the domain and the electric field outside the domain continue to decrease. When the velocity of the domain (v_{domain}) is equal to the drift velocity of electrons outside the domain, the domain stops growing. When the domain is absorbed, the output current will fluctuate, and new domains will be generated, thus forming periodic oscillations.

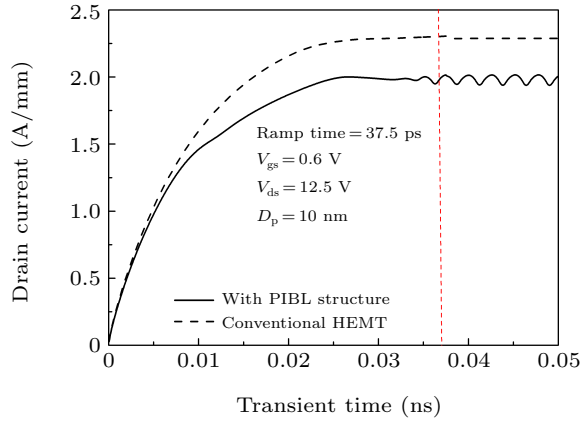


Fig. 3. Transient behavior of drain terminal current.

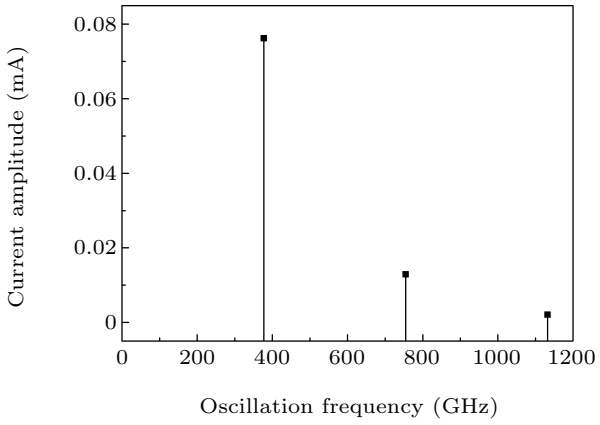


Fig. 4. Frequency spectrum of the oscillation drain current obtained by fast Fourier analysis.

The electron concentration distributions for both HEMTs are drawn in Fig. 6. The generation and movement of domains caused changes in the electron concentration in the PIBL region. For the PIBL structural HEMT, the gate acts as a hot electron injector that reduces the length of the "dead zone" and easily triggers the formation of electron domains. The results of the transient simulation show that it can generate a stable oscillation current and achieve the frequency of the fundamental wave up to 377 GHz, far higher than the f_T and f_{MAX} of conventional 0.2 μm gate GaN HEMTs.

The influence of N_p on the fundamental frequency of the device and the minimum V_{ds} required for generating stable oscillation is depicted in Fig. 7. With the increase of N_p from 2.5×10^{18} cm^{-3} to 3×10^{18} cm^{-3}, the electric field strength

of the PIBL region in the channel is more likely to meet the conditions required for domain generation, so that the minimum V_{ds} required for device operation decreases from 11.8 V to 10 V. In addition, it can be observed that the fundamental frequency decreases from 377 GHz to 344 GHz. As N_p increases, the p–n junction composed of the p-GaN island and the n-GaN buffer layer above the island depletes more 2DEG. The reduction of the channel electron concentration above the island forms a local high resistance region, which changes the electric field distribution in the channel. The electric field is mainly concentrated on the drain side of the PIBL structure. This changes the nucleation sites of the electronic domains and the distance from the electron domain nucleation point to the drain side of PIBL structure, which affects the device frequency.

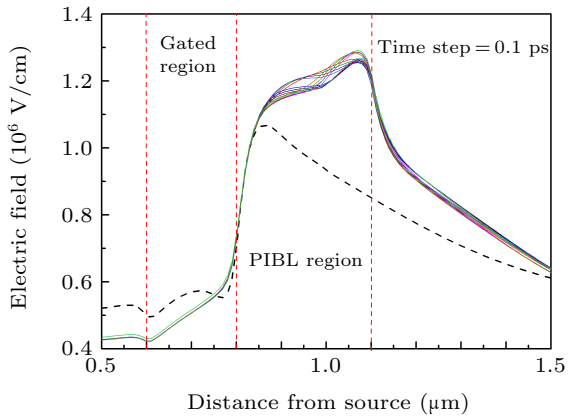


Fig. 5. Electric field distribution in 2DEG channel, where the time step is 0.1 ps for transient simulation. Solid lines are obtained from HEMT with PIBL, and dashed lines from HEMT without PIBL.

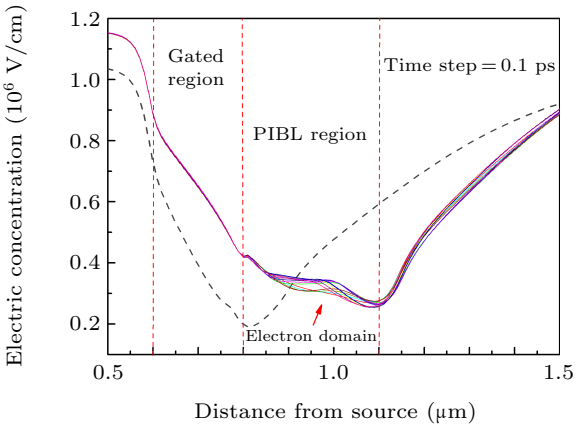


Fig. 6. Electron concentration distribution in the 2DEG channel, where the time step is 0.1 ps. Solid lines are obtained from HEMT with PIBL, and dashed lines from HEMT without PIBL.

The distance D_p between the p-GaN island and the heterojunction interface is a critical processing parameter of device fabrication since it significantly affects the performance of the device. In order to investigate the influence of D_p on the channel electric field and the oscillation characteristics, we select D_p from 5 nm to 15 nm for simulation. The results regarding D_p are shown in Fig. 8 under the bias of $V_{gs} = 0.6$ V, $V_{ds} = 12.5$ V. As D_p increases from 5 nm to 15 nm, the extracted oscillation frequency decreases from 400 GHz to 344 GHz. When $D_p = 5$ nm, excessively closing the PIBL region to the channel would make the island have a very strong depletion effect on the 2DEG channel. Although the high electric field above the PIBL region facilitates the transition of electrons from the low energy valley to the high energy valley, the too low electron concentration in the channel makes it difficult for the PIBL region to meet the conditions of electron domain formation. As a result, the oscillation frequency of 400 GHz and I_{rf}/I_{avg} of 3% are obtained due to the high electron domain velocity and narrow electron domain width. Similarly, for the sample with $D_p = 10$ nm, the higher electron concentration in the channel above PIBL contributes to electron accumulation, which increases the width of the electron domain and reduces the electron domain rate v_{domain}, thus reducing the fundamental frequency of the oscillating current but increasing the I_{rf}/I_{avg}. Also, a too-small D_p would cause Mg-dopant diffusing into the 2DEG channel and impact the operation of HEMT. Conversely, a too-large D_p suppresses the p-GaN island modulating the electric field of the channel, so that it is difficult to trigger the stable oscillation of the current. Therefore, it is necessary to adjust D_p according to the device process.

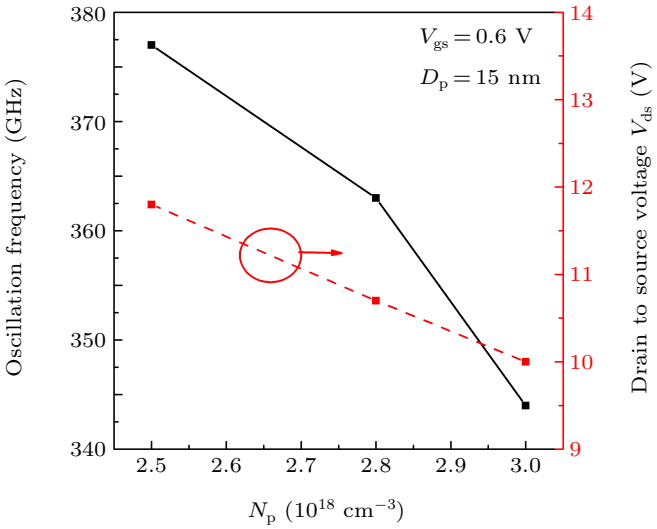


Fig. 7. Influence of N_p on the fundamental frequency and the minimum V_{ds} required for generating stable oscillation.

We also investigated the oscillation characteristics of HEMTs with two PIBLs, which are aimed at enhancing the higher-order harmonic components of the output current. The second p-GaN island is located between the first one and the drain. It obviously requires higher gate and drain biases to sustain a sufficient electric field strength and perturbation. Simulation results show that the device's operating mode is consistent with the aforementioned HEMT with one PIBL when V_{gs} is lower than 5 V. This means that the adjustment of the second island to the electric field of 2DEG channel is weak. As V_{gs}

increases to 5 V–6 V accompanied by V_{ds} approaching 29 V, the formation of Gunn domains appears at the position above the second island. In this case, the fundamental frequency of the oscillation current is around 100 GHz; concurrently, the fifth harmonic component exhibits a significant enhancement. However, an excessively higher gate voltage will cause a large leakage current, which negatively influences normal operation, even leading to a high risk of breakdown for HEMTs. Thus, it is difficult to use in actual circuits.

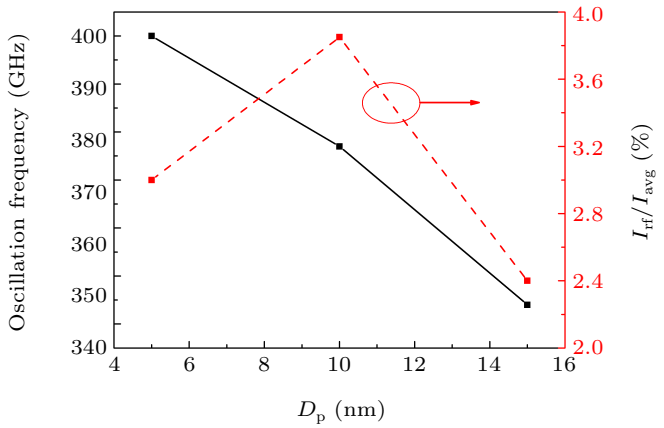


Fig. 8. Influence of D_p on the fundamental oscillation frequency and I_{rf}/I_{avg}, where $V_{gs} = 0.6$ V and $V_{ds} = 12.5$ V.

4. Conclusion

In this paper, we propose GaN-HEMTs with a PIBL structure and the oscillation mechanism of a drain current by using the numerical simulation on the Silvaco-TCAD platform. The simulation results show that the 0.2 μm gate HEMT with one PIBL can generate the stable oscillation of the drain current with a fundamental frequency up to 377 GHz at the low gate bias of $V_{gs} = 0.6$ V. The electric field distribution in HEMTs with a PIBL structure is more conducive to the formation of Gunn-like domains. The position of the PIBL structure significantly affects the oscillation frequency and the RF output power of the device. By appropriately increasing D_p, the influence of Mg diffusion on the 2DEG in the actual device can be reduced, although this reduces the oscillation frequency of the output current. At present, the RF output power of the device is relatively low, and it is difficult to meet the application requirements of actual circuits, but this kind of HEMT may reduce the requirements for device size and simplify the circuit scale of the THz system, therefore exhibiting great potential for THz applications compared with vertically structural Gunn diodes.

Acknowledgments

Project supported by the National Natural Science Foundation of China (Grant Nos. 61974108 and 61674117), the National Natural Science Foundation for Young Scholars of China (Grants No. 61804119), and the Postdoctoral Science Foundation of China (Grants No. 2018M643576).

References

[1] Pan J T, Wang Y, Xu K Y, Xiong J W and Tang Z L 2018 *Solid State Comm.* **271** 85
[2] Hong S M, Jang J H and Ieee 2016 *Joint International Eurosoi Workshop and International Conference on Ultimate Integration on Silicon*, (International Conference on Ultimate Integration on Silicon, 2016) pp. 250–253
[3] Shinohara K, Regan D C, Tang Y, Corrion A L, Brown D F, Wong J C, Robinson J F, Fung H H, Schmitz A, Oh T C, Kim S J, Chen P S, Nagele R G, Margomenos A D and Micovic M 2013 *IEEE T. Electron. Dev.* **60** 2982
[4] Zheng J X, Ma X H, Lu Y, Zhao B C, Zhang H H, Zhang M, Cao M Y and Hao Y 2015 *Chin. Phys. B* **24** 107305
[5] Dunn G M, Phillips A and Topham P 2001 *Electron. Lett.* **37** 530
[6] Wang Y, Yang L A, Mao W, Long S and Hao Y 2013 *IEEE T. Electron. Dev.* **60** 1600
[7] Ahi K 2017 *Opt. Eng.* **56** 090901
[8] Khalid A, Pilgrim N J, Dunn G M, Holland M C, Stanley C R, Thayne I G and Cumming D R S 2007 *IEEE T. Electron. Dev.* **28** 849
[9] Yang L A, Hao Y, Yao Q and Zhang J 2011 *IEEE T. Electron. Dev.* **58** 1076
[10] Íñiguez-de-la-Torre A, Íñiguez-de-la-Torre I, Mateos J, González T, SangaréP, Faucher M, Grimbert B, Brandli V, Ducournau G and Gaquière C 2012 *J. Appl. Phys.* **111** 113705
[11] Sokolov V N, Kim K W, Kochelap V A and Woolard D L 2005 *J. Appl. Phys.* **98** 064507
[12] Wang Y, Yang L A, Wang Z, Ao J and Hao Y 2016 *Semi. Sci. Tech.* **31** 025001
[13] Yue Y Z, Hu Z Y, Guo J, Sensale-Rodriguez B, Li G W, Wang R H, Faria F, Fang T, Song B, Gao X, Guo S P, Kosel T, Snider G, Fay P, Jena D and Xing H L 2012 *IEEE T. Electron. Dev.* **33** 988
[14] Dasgupta S, Nidhi, Brown D F, Wu F, Keller S, Speck J S and Mishra U K 2010 *Appl. Phys. Lett.* **96** 143504
[15] Mandal S, Agarwal A, Ahmadi E, Bhat K M, Ji D, Laurent M A, Keller S and Chowdhury S 2017 *IEEE T. Electron. Dev.* **38** 933
[16] Chowdhury S, Wong M H, Swenson B L and Mishra U K 2010 *IEEE, 68th Device Research Conference*, pp. 201–202
[17] Chowdhury S, Swenson B L and Mishra U K 2008 *IEEE T. Electron. Dev.* **29** 543
[18] Xing H L, Green D S, Yu H J, Mates T, Kozodoy P, Keller S, Denbaars S P and Mishra U K 2003 *Jpn. J. Appl. Phys.* **42** 50
[19] Li J Z, Lin J Y, Jiang H X, Salvador A, Botchkarev A and Morkoc H 1996 *Appl. Phys. Lett.* **69** 1474
[20] Chang Y L, Ludowise M, Lefforge D and Perez B 1999 *Appl. Phys. Lett.* **74** 688
[21] Greenlee J D, Feigelson B N, Anderson T J, Tadjer M J, Hite J K, Mastro M A, Eddy C R, Hobart K D and Kub F J 2014 *J. Appl. Phys.* **116** 063502
[22] Pong B J, Pan C J, Teng Y C, Chi G C, Li W H, Lee K C and Lee C H 1998 *J. Appl. Phys.* **83** 5992
[23] Hu Z Y, Nomoto K, Qi M, Li W S, Zhu M D, Gao X, Jena D and Xing H G 2017 *IEEE T. Electron. Dev.* **38** 1071
[24] Huang W, Khan T and Chow T P 2006 *J. Electron. Mater.* **35** 726
[25] Koblmüller G, Chu R, Raman A, Mishra U and Speck J 2010 *J. Appl. Phys.* **107** 043527
[26] Yu T H and Brennan K F 2002 *J. Appl. Phys.* **91** 3730
[27] Faraclas E W and Anwar A F M 2006 *Solid State Elec.* **50** 1051
[28] Du J F, Liu D, Zhao Z Q, Bai Z Y, Li L, Mo J H and Yu Q 2015 *Superlattices and Microstructures* **83** 251
[29] Yeluri R, Lu J, Hurni C A, Browne D A, Chowdhury S, Keller S, Speck J S and Mishra U K 2015 *Appl. Phys. Lett.* **106** 183502